Journal of Theoretical and Applied Mechanics, Sofia, Vol.55 (2025) pp. 325-342
SOLID MECHANICS

DYNAMICS OF AXIALLY MOVING PLATES IMMERSED IN FLUID SUBJECTED TO FOLLOWER FORCE

HONG YING LI*, QIN JING JI, MING YAO ZHANG, JIAN LI

Key Laboratory of Structural Dynamics of Liaoning Province,
College of Sciences, Northeastern University, Shenyang 110819, China

[Received: 9 July 2024. Accepted: 30 September 2025]

doi: https://doi.org/10.55787/jtams.25.55.3.325

ABSTRACT: The dynamics is investigated for an axially moving immersed plate subjected to time-dependent tension and follower force. The study is focused on simultaneous resonant cases i.e. principal parametric resonance and subharmonic resonance. Based on von Kármán plate theory and D'Alambert's principle, the vibration equations of the plate are derived. Employing the method of multiple scales, simultaneous resonance is discussed. Stability of periodic solutions of the system is examined by Lyapunov's stability theory. By analyzing the influence of follower load amplitude and tuning parameter on the steady-state periodic motion of simultaneous resonances, the system displays complex and variable dynamical behaviors. Furthermore, the approximate analytical results are verified by using the Runge-Kutta method.

KEY WORDS: Axially moving plates; Follower force; Simultaneous resonances; Stability.

1 INTRODUCTION

The axially moving structures are commonly found in manufacturing and industrial engineering fields such as conveyor belts, wire cutting machining, elevator transmission cables and steel strips in a steel sheet production line, etc. In some mechanical systems, axially moving components are the main source of vibration; for this reason, dynamic characteristics of such systems have been studied for many years [1–7].

Nonlinear vibration of axially moving systems exists in a number of industrial applications. Some references [8–11] studied the nonlinear dynamic behavior of such systems, like forced resonance, internal resonance and combined resonance. Pakdemirli and Öz [12] analyzed the transverse vibrations of simply supported axially moving Euler–Bernoulli beams, and performed the detailed analysis of the resonances. Ghayesh [13] investigated the forced dynamics of an axially moving viscoelastic beam and presented the amplitude-frequency responses and bifurcation diagrams of Poincaré maps for several values of the system parameters. Mao et al. [14]

*Corresponding author e-mail: lihy@mail.neu.edu.cn

used the method of multiple scales to study internal and forced resonances of an axially moving beam. Tang and Chen [15] used analytical and numerical methods to study the steady-state responses of in-plane translating viscoelastic plates in external and internal resonances. Zhou and Wang [16] investigated the transverse vibration and dynamic stability of the axially moving viscoelastic plate and analyzed the variation relationship between the first three complex frequencies of the system and the dimensionless axially moving speed with different aspect ratio and dimensionless delay time. Lu et al. [17] studied the dynamic stability of an axially moving graphene reinforced laminated composite plate and evaluated the stability of the system. Considering different boundary conditions, Song and She [18] studied the nonlinear resonance behavior of axially moving graphene platelets reinforced metal foams plates with geometric imperfection, and discussed the effects of different boundary conditions, material properties, geometric imperfection, and axial velocity on the resonance of the plate.

For axially moving structures, time-dependent axial velocity and tension can cause complex parameter vibrations. For example, Ghayesh [19] examined the coupled longitudinal–transverse nonlinear dynamics of an axially accelerating beam, where the axial speed is assumed to be comprised of a constant mean value along with harmonic fluctuations. Tang et al. [20] investigated parametric and 3:1 internal resonance of axially moving viscoelastic beams on elastic foundation. The paper carried out a detailed study to determine the influence of the viscoelastic coefficient and the viscous damping coefficient on dynamic behavior of the system. Mao et al. [21] employed the method of multiple scales to study steady-state responses of an axially moving beam subjected to parametric combined with forced excitations. Sahoo et al. [22–24] applied analytical and numerical approach to find the steady-state and dynamic behaviors of an axially accelerating viscoelastic beam subject to two-frequency parametric excitation in presence of internal resonance, and studied the effect of variations of fluctuating tension component, fluctuating velocity component independently and when combined, internal and parametric frequency detuning parameters and damping on the traveling viscoelastic beam. Zhang et al. [25] investigated nonlinear transverse vibrations of in-plane accelerating viscoelastic plates with a varying tension in the presence of principal parametric and 3:1 internal resonance.

In above-mentioned researches, the dynamics researches of the axially moving structures are based on the manufacturing and engineering backgrounds. Therefore, in practical applications, the axially moving structures may locate in particular environment or subjected to special load, leading to complex nonlinear dynamic behaviors. For example, Hu and Zhang [26] investigated nonlinear parametric vibration and stability of an axially accelerating rectangular thin plate subjected to parametric excitations resulting from the axial time-varying tension and axial time-varying

speed in the magnetic field. Yao et al. [27] studied the nonlinear primary resonances of an axially moving plate in aero-thermal environment concerning on manufacturing background of the hot rolling. Wang et al. [28] analyzed vibration and stability of an axially moving beam in fluid by introducing the "axial added mass coefficient". Yao et al. [29] investigated dynamics and stability of an axially moving beam subjected to axial flows, and indicated that the beam loses stability via buckling or flutter at a critical speed of moving beam which is associated with variations of system parameters. Wang et al. [30] developed an efficient method to study the vibration and stability of moving plates immersed in fluid by applying the Kirchhoff plate theory and finite element method. Guo et al. [31] investigated the dynamic characteristics and stability of the moving thermoelastic coupling rectangular plate subjected to uniformly distributed tangential follower force. Wang et al. [32] analyzed the stability of the moving viscoelastic plate with the piezoelectric layer subjected to uniformly distributed tangential follower force.

In this paper, the studying model originates from the hot-dip galvanizing production line in the steel industry (Fig. 1). Literatures [33–35] studied the influence of fluid parameters on the vibration characteristics of the plate coupled with fluid. Therefore, the focus of this paper is applied on the nonlinear dynamic behaviors of axially moving immersed plates subjected to time-varying tension and follower force. The governing partial-differential equation of motion of the plate is developed, then is discretized using Galerkin's technique. For the time-variant tension case, the method of multiple scales and Runge Kutta method are employed to analyze parametric and subharmonic simultaneous resonances.

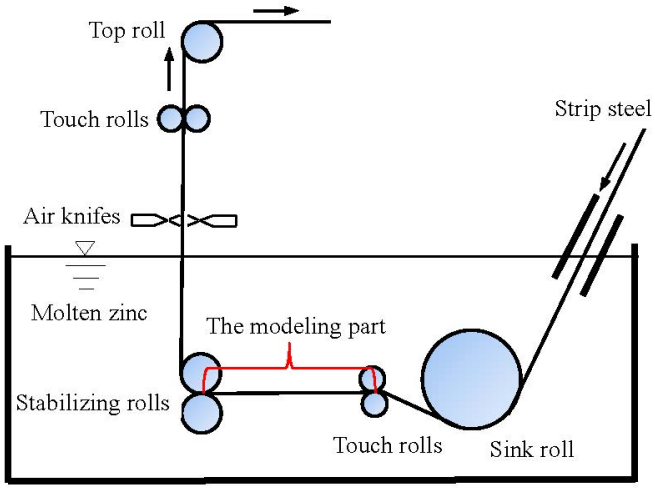

Fig. 1. Continuous hot-dip galvanizing production line.

2 GOVERNING EQUATION

The paper simplifies the research model derived from the continuous hot-dip galvanizing process (Fig. 1) to moving rectangular plates submerged in fluid (Fig. 2). Under in-plane time-varying tension $F_x(t)$, the plate is moving with a speed V in the x direction, and subjected to follower force F_Q. The plate has the length a, width b and thickness h in x, y and z directions, respectively. The density of the plate is ρ, Young's modulus is E, Poisson's ration is μ, damping coefficient is c. The density of the fluid is ρ_f. Displacements of the mid-plane of the plate are $u = u(x, y, t)$, $v = v(x, y, t)$ and $w = w(x, y, t)$ in the x, y and z directions from the static equilibrium ($u = v = w = 0$), respectively.

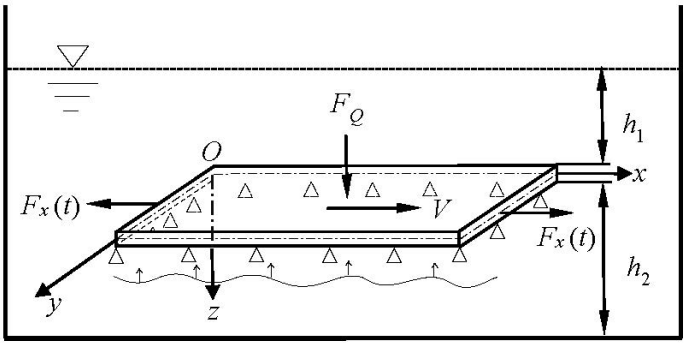

Fig. 2. Axially moving immersed plates subjected to follower force.

According to the von Kármán nonlinear plate theory, the following relations, between the strain of a generic point of the plate and the displacement field, are given [36]:

$$
\begin{aligned}
\varepsilon_x &= \frac{\partial u}{\partial x} + \frac{1}{2}\left(\frac{\partial w}{\partial x}\right)^2 - z\frac{\partial^2 w}{\partial x^2} \\
\varepsilon_y &= \frac{\partial v}{\partial y} + \frac{1}{2}\left(\frac{\partial w}{\partial y}\right)^2 - z\frac{\partial^2 w}{\partial y^2} \\
\gamma_{xy} &= \frac{\partial u}{\partial y} + \frac{\partial v}{\partial x} + \frac{\partial w}{\partial x}\frac{\partial w}{\partial y} - 2z\frac{\partial^2 w}{\partial x \partial y}
\end{aligned}
\tag{1}
$$

The relations between the stresses and strains for homogeneous and isotropic materials may be written as

$$\begin{aligned}\sigma_x &= \frac{E}{1-\mu^2}(\varepsilon_x + \mu\varepsilon_y)\,,\\ \sigma_y &= \frac{E}{1-\mu^2}(\varepsilon_y + \mu\varepsilon_x)\,,\\ \tau_{xy} &= \frac{E}{2(1+\mu)}\gamma_{xy}\,.\end{aligned} \tag{2}$$

The force and moment resultants can be expressed as

$$\begin{aligned}N_x &= \int_{-\frac{h}{2}}^{\frac{h}{2}} \sigma_x \mathrm{d}z \quad N_y = \int_{-\frac{h}{2}}^{\frac{h}{2}} \sigma_y \mathrm{d}z \quad N_{xy} = \int_{-\frac{h}{2}}^{\frac{h}{2}} \tau_{xy}\mathrm{d}z\,,\\ M_x &= \int_{-\frac{h}{2}}^{\frac{h}{2}} \sigma_x z \mathrm{d}z \quad M_y = \int_{-\frac{h}{2}}^{\frac{h}{2}} \sigma_y z \mathrm{d}z \quad M_{xy} = \int_{-\frac{h}{2}}^{\frac{h}{2}} \tau_{xy} z\mathrm{d}z\,.\end{aligned} \tag{3}$$

The plate considered here is coupled with fluid, which is assumed to be inviscid and incompressible, and the motion is irrotational. According to D'Alambert's principle, the equation of nonlinear vibration of the axially moving plate is obtained as

$$\begin{aligned}\rho h\frac{\mathrm{d}^2 w}{\mathrm{d}t^2} - F_x(t)\frac{\partial^2 w}{\partial x^2} + c\frac{\mathrm{d}w}{\mathrm{d}t} - \frac{\partial^2 M_x}{\partial x^2} - \frac{\partial^2 M_y}{\partial y^2} - 2\frac{\partial^2 M_{xy}}{\partial x \partial y}\\ - N_x\frac{\partial^2 w}{\partial x^2} - 2N_{xy}\frac{\partial^2 w}{\partial x \partial y} - N_y\frac{\partial^2 w}{\partial y^2} - P_p = F_Q\,,\end{aligned} \tag{4}$$

where $P_p = m_{\text{add}}\Big(\dfrac{\partial^2 w}{\partial t^2} + V\dfrac{\partial^2 w}{\partial x \partial t}\Big)$. P_p indicates the dynamic pressure of fluid, which is transformed from the effect of interaction between fluid and plate by applying the velocity potential function and Bernoulli's equation. P_p can be solved by the method introduced in [37]. m_{add} is the added mass of fluid.

For axially moving plates, the total derivative can be expressed as

$$\begin{aligned}\frac{\mathrm{d}}{\mathrm{d}t} &= \frac{\partial}{\partial t} + V\frac{\partial}{\partial x}\,,\\ \frac{\mathrm{d}^2}{\mathrm{d}t^2} &= \frac{\partial^2}{\partial t^2} + 2V\frac{\partial^2}{\partial x \partial t} + V^2\frac{\partial^2}{\partial x^2}\,.\end{aligned} \tag{5}$$

In this paper, the follower force and the time-varying tension can be given as

$$\begin{cases} F_Q = Q\delta(x - Vt,\, y - y_0)\\ F_x(t) = F_{x_0} + F_{x_1}\cos(\Omega_1 t)\end{cases} \tag{6}$$

$$\delta(x - Vt,\, y - y_0) = \begin{cases} 1, & x = Vt,\, y = y_0 \\ 0, & \text{others} \end{cases} \tag{7}$$

where Q is the amplitude of follower force, F_{x_0} is the mean axial tension, F_{x_1} is the amplitude, and Ω_1 is the frequency of the harmonically varying components.

Introducing stress function Φ

$$\sigma_x = \frac{\partial^2 \Phi}{\partial y^2}, \quad \sigma_y = \frac{\partial^2 \Phi}{\partial x^2}, \quad \tau_{xy} = -\frac{\partial^2 \Phi}{\partial x \partial y}. \tag{8}$$

By the relations between the strains and the displacements (Eq. (1)), coordinated equation is constructed as

$$\frac{\partial^2 \varepsilon_x}{\partial y^2} + \frac{\partial^2 \varepsilon_y}{\partial x^2} - \frac{\partial^2 \gamma_{xy}}{\partial x \partial y} = \left(\frac{\partial^2 w}{\partial x \partial y}\right)^2 - \frac{\partial^2 w}{\partial x^2}\frac{\partial^2 w}{\partial y^2} \tag{9}$$

Substituting Eq. (2) and Eq. (8) into Eq. (9), meanwhile, substituting Eqs. (1)–(3) and Eqs. (5)–(6) into Eq. (4), one can obtain

$$\left(\frac{\partial^4 \Phi}{\partial x^4} + 2\frac{\partial^4 \Phi}{\partial x^2 \partial y^2} + \frac{\partial^4 \Phi}{\partial y^4}\right) = -E\left[\frac{\partial^2 w}{\partial x^2}\frac{\partial^2 w}{\partial y^2} - \left(\frac{\partial^2 w}{\partial x \partial y}\right)^2\right] \tag{10a}$$

$$\begin{aligned} D\nabla^2\nabla^2 w + \rho h\left(\frac{\partial^2 w}{\partial t^2} + 2V\frac{\partial^2 w}{\partial x \partial t} + V^2\frac{\partial^2 w}{\partial x^2}\right) \\ - \left[F_{x_0} + F_{x_1}\cos(\Omega_1 t)\right]\frac{\partial^2 w}{\partial x^2} + c\left(\frac{\partial w}{\partial t} + V\frac{\partial w}{\partial x}\right) \\ = h\left(\frac{\partial^2 \Phi}{\partial y^2}\frac{\partial^2 w}{\partial x^2} + \frac{\partial^2 \Phi}{\partial x^2}\frac{\partial^2 w}{\partial y^2} - 2\frac{\partial^2 \Phi}{\partial x \partial y}\frac{\partial^2 w}{\partial x \partial y}\right) \\ + m_{\text{add}}\left(\frac{\partial^2 w}{\partial t^2} + V\frac{\partial^2 w}{\partial x \partial t}\right) + Q\delta(x - Vt, y - y_0) \end{aligned} \tag{10b}$$

where $D = Eh^3/[12(1-\mu^2)]$.

Introduce following dimensionless parameters and variables

$$\begin{aligned} &\overline{x} = \frac{x}{a}, \quad \overline{y} = \frac{y}{b}, \quad \overline{w} = \frac{w}{h}, \quad \xi = \frac{a}{b}, \quad \tau = t\sqrt{\frac{D}{\rho h a^4}}, \\ &\overline{V} = V\sqrt{\frac{\rho h a^2}{D}}, \quad \overline{m} = \frac{m_{\text{add}}}{\rho h}, \quad \overline{c} = c\sqrt{\frac{a^4}{D\rho h}}, \quad \overline{\Phi} = \frac{\Phi}{Eh^2}, \\ &\overline{F}_Q = \frac{a^4 Q}{Dh}, \quad \overline{F}_{x_0} = \frac{F_{x_0} a^2}{D}, \quad \overline{F}_{x_1} = \frac{F_{x_1} a^2}{D}, \quad \overline{\Omega}_1 = \Omega_1\sqrt{\frac{\rho h a^4}{D}} \end{aligned} \tag{11}$$

Introducing Eq. (11) into Eq. (10) gives the dimensionless equations

$$\left(\frac{\partial^4\overline{\Phi}}{\partial\overline{x}^4}+2\xi^2\frac{\partial^4\overline{\Phi}}{\partial\overline{x}^2\partial\overline{y}^2}+\xi^4\frac{\partial^4\overline{\Phi}}{\partial\overline{y}^4}\right)=\xi^2\left[\left(\frac{\partial^2\overline{w}}{\partial\overline{x}\partial\overline{y}}\right)^2-\frac{\partial^2\overline{w}}{\partial\overline{x}^2}\frac{\partial^2\overline{w}}{\partial\overline{y}^2}\right] \tag{12a}$$

$$\begin{aligned}&\left(\frac{\partial^4\overline{w}}{\partial\overline{x}^4}+2\xi^2\frac{\partial^4\overline{w}}{\partial\overline{x}^2\partial\overline{y}^2}+\xi^4\frac{\partial^4\overline{w}}{\partial\overline{y}^4}\right)+\left(\frac{\partial^2\overline{w}}{\partial\tau^2}+2\overline{V}\frac{\partial^2\overline{w}}{\partial\overline{x}\partial\tau}+\overline{V}^2\frac{\partial^2\overline{w}}{\partial\overline{x}^2}\right)\\&-[\overline{F}_{x_0}+\overline{F}_{x_1}\cos(\overline{\Omega}_1\tau)]\frac{\partial^2\overline{w}}{\partial\overline{x}^2}+\overline{c}\left(\frac{\partial\overline{w}}{\partial\tau}+\overline{V}\frac{\partial\overline{w}}{\partial\overline{x}}\right)-\overline{m}\left(\frac{\partial^2\overline{w}}{\partial\tau^2}+\overline{V}\frac{\partial^2\overline{w}}{\partial\overline{x}\partial\tau}\right)\\&=12(1-\mu^2)\xi^2\left(\frac{\partial^2\overline{w}}{\partial\overline{x}^2}\frac{\partial^2\overline{\Phi}}{\partial\overline{y}^2}+\frac{\partial^2\overline{w}}{\partial\overline{y}^2}\frac{\partial^2\overline{\Phi}}{\partial\overline{x}^2}-2\frac{\partial^2\overline{w}}{\partial\overline{x}\partial\overline{y}}\frac{\partial^2\overline{\Phi}}{\partial\overline{x}\partial\overline{y}}\right)\\&+\overline{F}_Q\delta(\overline{x}-\overline{V}\tau,\overline{y}-\overline{y}_0)\end{aligned} \tag{12b}$$

The dimensionless boundary conditions of the plate with four edges simply supported are as follows:

$$\overline{w}\Big|_{\overline{x}=0}=\overline{w}\Big|_{\overline{x}=1}=\overline{w}\Big|_{\overline{y}=0}=\overline{w}\Big|_{\overline{y}=1}=0\,, \tag{13a}$$

$$\frac{\partial^2\overline{w}}{\partial\overline{x}^2}\Big|_{\overline{x}=0}=\frac{\partial^2\overline{w}}{\partial\overline{x}^2}\Big|_{\overline{x}=1}=\frac{\partial^2\overline{w}}{\partial\overline{y}^2}\Big|_{\overline{y}=0}=\frac{\partial^2\overline{w}}{\partial\overline{y}^2}\Big|_{\overline{y}=1} \tag{13b}$$

Through analytical and numerical analysis, it is found that the axially moving immersed plate subjected to time-varying tension and follower force exhibits complex dynamic characteristics. This paper mainly focuses the first mode (m =1, n =1), and more complex mode interactions will be discussed in subsequent work. According to the four-edge simply supported boundary condition, the displacement function can be given

$$\overline{w}(\overline{x},\overline{y},\tau)=q_{11}(\tau)\sin(\pi\overline{x})\sin(\pi\overline{y})\,. \tag{14}$$

Substitute Eq. (14) into the first equation of Eq. (12), dimensionless stress function is obtained

$$\overline{\Phi}=q_{11}^2(A_1\cos 2\pi\overline{x}+A_2\cos 2\pi\overline{y})+\frac{1}{2}P_x\overline{y}^2+\frac{1}{2}P_y\overline{x}^2\,, \tag{15}$$

where $A_1=\xi^2/32$, $A_2=1/(32\xi^2)$.

Considering a thin plate with four-edge simply supported, the dimensionless expressions for the relative distance of the two opposite sides of the plate can be obtained by Eq. (1), Eq. (2), Eq. (8), Eq. (14) and Eq. (15)

$$\int_0^1\int_0^1\left[\left(\xi^2\frac{\partial^2\overline{\Phi}}{\partial\overline{y}^2}-\mu\frac{\partial^2\overline{\Phi}}{\partial\overline{x}^2}\right)-\frac{1}{2}\left(\frac{\partial\overline{w}}{\partial\overline{x}}\right)^2\right]\mathrm{d}\overline{x}\mathrm{d}\overline{y}=0\,, \tag{16a}$$

$$\int_0^1\int_0^1\Big[\Big(\frac{\partial^2\overline{\Phi}}{\partial\overline{x}^2}-\mu\xi^2\frac{\partial^2\overline{\Phi}}{\partial\overline{y}^2}\Big)-\frac{1}{2}\xi^2\Big(\frac{\partial\overline{w}}{\partial\overline{y}}\Big)^2\Big]\mathrm{d}\overline{x}\mathrm{d}\overline{y}=0\,. \tag{16b}$$

Substitute Eq. (14) and Eq. (15) into Eq. (16), one can obtain

$$P_x=\frac{\pi^2(1+\mu\xi^2)q_{11}^2}{8(1-\mu^2)\xi^2}\,,\qquad P_y=\frac{\pi^2(\xi^2+\mu)q_{11}^2}{8(1-\mu^2)}\,. \tag{17}$$

Substituting Eq. (7), Eq. (14), Eq. (15) and Eq. (17) into the second expression of Eq. (12), the nonlinear differential equations (Eq. (18)) on modal coordinates are achieved using the Galerkin integration

$$\begin{aligned}\ddot{q}_{11}=d_1\dot{q}_{11}+d_2q_{11}+d_3(\overline{F}_{x_0}-\overline{V}^2)q_{11}\\+d_3\overline{F}_{x_1}\cos(\overline{\Omega}_1\tau)q_{11}+d_4q_{11}^3+d_5\overline{F}_Q\sin(\overline{\Omega}_2\tau)\,,\end{aligned} \tag{18}$$

where the over-dot means derivative with respect to τ,

$$d_1=\frac{\bar{c}}{-1+\overline{m}}\,,\quad d_2=\frac{\pi^4+2\pi^4\xi^2+\pi^4\xi^4}{-1+\overline{m}}\,,\quad d_3=\frac{\pi^2}{-1+\overline{m}}\,,$$
$$d_4=-\frac{3\pi^4(3-\mu)(1+\mu)}{2(1+\overline{m})}\,,\quad d_5=\frac{3\pi^4(3-\mu^2+4\mu\xi^2+3\xi^4-\mu^2\xi^4)}{4(-1+\overline{m})}\,,\quad \overline{\Omega}=\pi\overline{V}\,.$$

3 Solution Procedure

The method of multiple scales [38–40] is used to solve the nonlinear equation. For the procedures of multiple scales method, Eq. (18) can be rewritten

$$\ddot{q}_{11}+\omega_{11}^2q_{11}=\varepsilon(s_1\dot{q}_{11}+s_2q_{11}+s_3q_{11}\overline{F}_{x_1}\cos(\overline{\Omega}_1\tau)+s_4q_{11}^3)+d_5\overline{F}_Q\sin(\overline{\Omega}_2\tau)\,, \tag{19}$$

where ε is a small dimensionless parameter, ω_{11} is the first dimensionless natural frequency of the system, $s_i=d_i/\varepsilon$ $(i=1,3,4)$, $s_2=(d_2+d_3(\overline{F}_{x_0}-\overline{V}^2)+\omega_{11}^2)/\varepsilon$. Time scales are defined as $T_r=\varepsilon^r\tau$ $(r=0,1)$. Therefore,

$$\frac{\mathrm{d}}{\mathrm{d}\tau}=D_0+\varepsilon D_1+O(\varepsilon^2)\,,\quad \frac{\mathrm{d}^2}{\mathrm{d}\tau^2}=D_0^2+2\varepsilon D_0D_1+O(\varepsilon^2)\,, \tag{20}$$

in which $D_0=\partial/\partial T_0$, $D_1=\partial/\partial T_1$.

According to the method of multiple scales, the approximate solution for Eq. (19) can be expressed in terms of different time scales as

$$q_{11}(t)=q_1(T_0,T_1)+\varepsilon q_2(T_0,T_1)\,. \tag{21}$$

Substituting Eqs. (20) and (21) into Eq. (19), then equating the coefficients of ε^0 and ε^1 at both sides, it yields

• Order of ε^0

$$D_0^2 q_1 + q_1 \omega_{11}^2 = d_5 \overline{F}_Q \sin(\overline{\Omega}_2 T_0)\,. \tag{22}$$

• Order of ε^1

$$D_0^2 q_2 + \omega_{11}^2 q_2 = -2D_0 D_1 q_1 + s_1 D_0 q_1 + s_2 q_1 + s_3 q_1 \overline{F}_{x_1} \cos(\overline{\Omega}_1 T_0) + s_4 q_1^3\,. \tag{23}$$

The solution of Eq. (22) can be written as

$$\begin{aligned} q_1(T_0, T_1) &= a_1(T_1)\cos[\omega_1 T_0 + \beta_1(T_1)] + 2B\sin(\overline{\Omega}_2 \tau) \\ &= A(t)\mathrm{e}^{i\omega_{11}T_0} + iB\mathrm{e}^{i\overline{\Omega}_2 T_0} + cc\,, \end{aligned} \tag{24}$$

where $a_1(T_1)$ and $\beta_1(T_1)$ are amplitude and phase respectively,

$$A(T_1) = a_1(T_1)\mathrm{e}^{i\beta_1(T_1)}/2\,, \qquad B = (d_5\overline{F}_Q)/(2\omega_{11}^2 - 2\overline{\Omega}_2^2)\,,$$

cc denotes the complex conjugate of the preceding terms.

In this section, simultaneous resonant cases, namely principal parametric resonance and subharmonic resonance, are investigated. The detuning parameters σ_1 and σ_2 are introduced to define principal parametric resonance and subharmonic resonance, respectively,

$$\Omega_1 = 2\omega_{11} + \varepsilon\sigma_1\,, \quad \Omega_2 = 3\omega_{11} + \varepsilon\sigma_2\,. \tag{25}$$

Substituting Eq. (24) and Eq. (25) into Eq. (23), one gets

$$\begin{aligned} D_1 a_1 = {} & \frac{s_1 a_1}{2} - \frac{s_3 \overline{F}_{x_1} a_1 \sin(2\beta_1 - \sigma_1 T_1)}{4\omega_1} \\ & + \frac{s_3 B \overline{F}_{x_1} \cos(\beta_1 + \sigma_1 T_1 - \sigma_2 T_1)}{2\omega_1} + \frac{3 s_4 B a_1^2 \cos(3\beta_1 - \sigma_2 T_1)}{4\omega_1}\,, \end{aligned} \tag{26a}$$

$$\begin{aligned} a_1 D_1 \beta_1 = {} & -\frac{s_2 a_1}{2\omega_1} - \frac{s_3 \overline{F}_{x_1} a_1 \cos(2\beta_1 - \sigma_1 T_1)}{4\omega_1} \\ & - \frac{s_3 B \overline{F}_{x_1} \sin(\beta_1 + \sigma_1 T_1 - \sigma_2 T_1)}{2\omega_1} - \frac{3 s_4 a_1^3}{8\omega_1} \\ & - \frac{3 s_4 B^2 a_1}{\omega_1} - \frac{3 s_4 B a_1^2 \sin(3\beta_1^2 - \sigma_2 T_1)}{4\omega_1}\,. \end{aligned} \tag{26b}$$

By analyzing equation Eq. (26), it can be seen that for steady-state response ($D_1 a_1 = 0$ and $D_1 \beta_1 = 0$), $(\beta_1 + \sigma_1 T_1 - \sigma_2 T_1)$, $(2\beta_1 - T_1 \sigma_1)$ and $(3\beta_1 - \sigma_2 T_1)$ in Eq. (26) are all constants, this means $D_1 \beta_1 = \sigma_2 = 3\sigma_1/2$. Letting $\gamma_1 = \beta_1 + \sigma_1 T_1 - \sigma_2 T_1$, one gets nonlinear equations

$$D_1 a_1 = \frac{s_1 a_1}{2} - \frac{s_3 \overline{F}_{x_1} a_1 \sin 2\gamma_1}{4\omega_1} + \frac{s_3 B \overline{F}_{x_1} \cos \gamma_1}{2\omega_1} + \frac{3 s_4 B a_1^2 \cos 3\gamma_1}{4\omega_1}, \tag{27a}$$

$$D_1 \gamma_1 = -\frac{\sigma_2}{3} - \frac{s_2}{2\omega_1} - \frac{s_3 \overline{F}_{x_1} \cos 2\gamma_1}{4\omega_1} - \frac{s_3 B \overline{F}_{x_1} \sin \gamma_1}{2\omega_1 a_1} - \frac{3 s_4 a_1^2}{8\omega_1} - \frac{3 s_4 B^2}{\omega_1} - \frac{3 s_4 B a_1 \sin 3\gamma_1}{4\omega_1}. \tag{27b}$$

The approximately analytical solution of Eq. (27) can be expressed as

$$q_{11}(\tau) = a_1 \cos\left(\frac{1}{3}\overline{\Omega}_2 \tau + \gamma_1\right) + 2B \sin(\overline{\Omega}_2 \tau), \tag{28}$$

where a and γ are determined by Eq. (27).

Letting $D_1 a_1 = 0$ and $D_1 \gamma_1 = 0$ in Eq. (27), one can obtain steady-state response for the system.

To study the stability of the steady-state solution, a state vector $\mathbf{Z} = [a, \gamma]^{\mathrm{T}}$ is defined, then the vector function can be constructed from Eq. (27) as

$$\mathbf{F}(\mathbf{Z}) = \dot{\mathbf{Z}} = \tag{29}$$

$$\begin{bmatrix} \dfrac{s_1 a_1}{2} - \dfrac{s_3 \overline{F}_{x_1} a_1 \sin 2\gamma_1}{4\omega_1} + \dfrac{s_3 B \overline{F}_{x_1} \cos \gamma_1}{2\omega_1} + \dfrac{3 s_4 B a_1^2 \cos 3\gamma_1}{4\omega_1} \\ -\dfrac{\sigma_2}{3} - \dfrac{s_2}{2\omega_1} - \dfrac{s_3 \overline{F}_{x_1} \cos 2\gamma_1}{4\omega_1} - \dfrac{s_3 B \overline{F}_{x_1} \sin \gamma_1}{2\omega_1 a_1} - \dfrac{3 s_4 a_1^2}{8\omega_1} - \dfrac{3 s_4 B^2}{\omega_1} - \dfrac{3 s_4 B a_1 \sin 3\gamma_1}{4\omega_1} \end{bmatrix}$$

The Jacobi matrix of $\mathbf{F}(\mathbf{Z})$ is

$$\mathbf{J} = \begin{bmatrix} J_{11} & J_{12} \\ J_{21} & J_{22} \end{bmatrix}, \tag{30}$$

where

$$J_{11} = \frac{s_1}{2} - \frac{s_3 \overline{F}_{x_1} \sin 2\gamma_1}{4\omega_1} + \frac{3 s_4 B a_1 \cos 3\gamma_1}{4\omega_1},$$

$$J_{12} = -\frac{s_3 \overline{F}_{x_1} a_1 \cos 2\gamma_1}{2a_1} - \frac{s_3 B \overline{F}_{x_1} \sin \gamma_1}{2\omega_1} - \frac{9 s_4 B a_1^2 \sin 3\gamma_1}{4\omega_1},$$

$$J_{21} = \frac{s_3 B \overline{F}_{x_1} \sin \gamma_1}{2\omega_1 a_1^2} - \frac{3 s_4 a_1}{8\omega_1} - \frac{3 s_4 B \sin 3\gamma_1}{4\omega_1},$$

$$J_{22} = \frac{s_3 \overline{F}_{x_1} \sin 2\gamma_1}{2\omega_1} - \frac{s_3 B \overline{F}_{x_1} \cos \gamma_1}{2\omega_1 a_1} - \frac{9 s_4 B a_1 \cos 3\gamma_1}{4\omega_1} .$$

The characteristic equation of Jacobi matrix of $\mathbf{F}(\mathbf{Z})$ is

$$\lambda^2 + S\lambda + H = 0 , \tag{31}$$

where $S = \mathrm{Tr}\,(\mathbf{J})$, $h = \det(\mathbf{J})$, and λ is the eigenvalue.

According to Lyapunov's stability theory, when all eigenvalues of the Jacobi matrix have negative real parts, the steady-state solution is stable, otherwise it is unstable.

4 Results and Discussions

Take the axially moving plate submerged in fluid as an example. The main parameters are as follows: $a = 1$ m, $b = 1$ m, $h = 1$ mm, $\rho = 7.85 \times 10^3$ kg/m^3, $\rho_f = 1.0 \times 10^3$ kg/m^3, $E = 207$ GPa, $\mu = 0.3$. Unless otherwise specified, the fixed parameters are selected as follows: $\omega_{11} = 3.95$, $\xi = 1$, $y_0 = 0.5b$, $\varepsilon = 0.01$, $F_Q = 336$, $F_{x_0} = 53$ and $F_{x_1} = -5.3$.

To verify the correctness and accuracy of the analytical solutions obtained by Eq. (28), the fourth-order Runge-Kutta method is applied to solve Eq. (18). As shown in Fig. 3, the analytical solution exhibits good agreement with numerical results.

For the steady-state response, amplitude-frequency curves (Fig. 4a) and phase-frequency curves (Fig. 4b) of simultaneous resonances are obtained by solving Eq. (27). To judge the stability of system's periodic solutions, Lyapunov's stability theory is applied by solving the eigenvalue of Eq. (31). It can be noticed that the system can

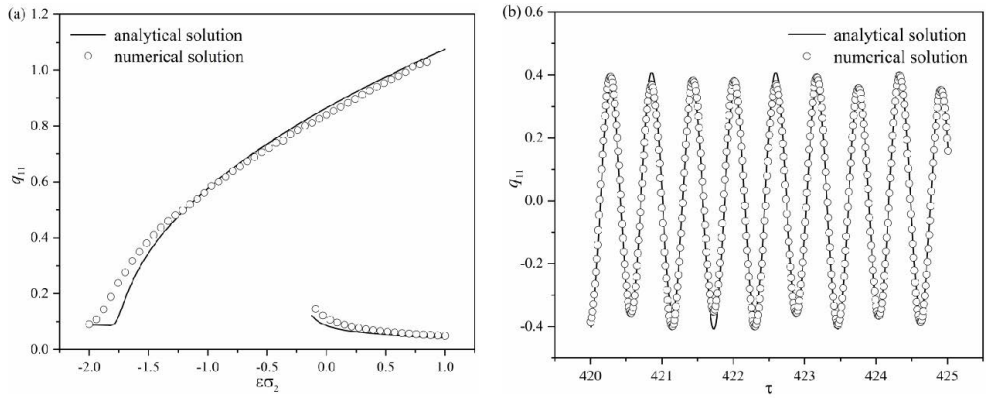

Fig. 3. Comparison of amplitude-frequency response and steady-state response: (a) amplitude- frequency response; (b) steady-state response.

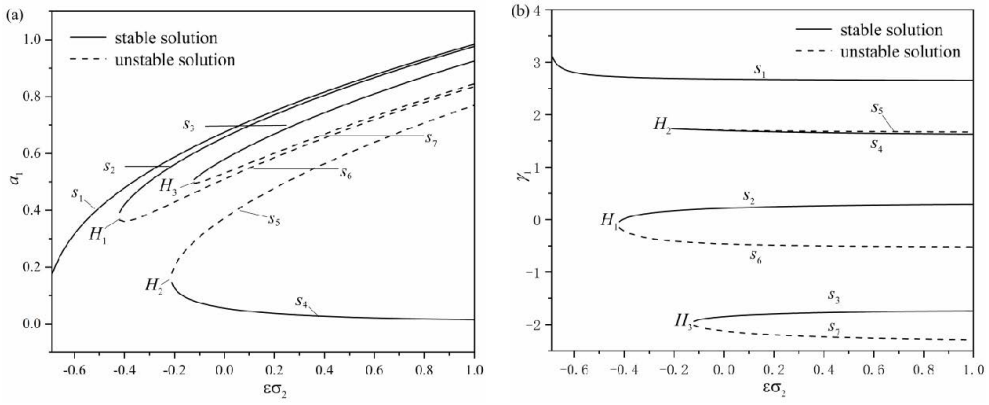

Fig. 4. Simultaneous resonance response curves: (a) amplitude-frequency curves; (b) phase-frequency curves.

have up to three bifurcation points (H_1, H_2 and H_3), which means the number and stability of periodic solutions change at these points. The amplitude-frequency response (Fig. 4a) contains as many as seven branches, namely s_1, s_2, s_3, s_4, s_5, s_6 and s_7. Among them, s_1, s_2, s_3 and s_4 are stable solution branches, while s_5, s_6 and

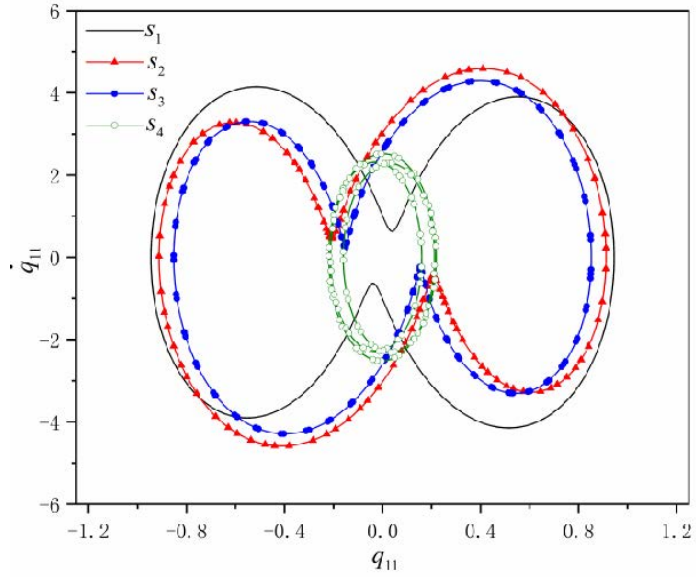

Fig. 5. Stable periodic orbits ($\overline{F}_Q = 336$, $\varepsilon\sigma_2 = 0.2$).

s_7 are unstable solution branches. Further analysis indicates that solution branches s_1, s_4 and s_5 display subharmonic resonance characteristics, s_2 and s_6 exhibit principal parameter resonance characteristics. However, s_3 and s_7 represent coupled resonances when simultaneous resonances of subharmonic resonances and principal parametric resonances occurs to the system.

Taking $\varepsilon\sigma_2 = 0.2$ as an example, the periodic orbits of four stable solutions (s_1, s_2, s_3 and s_4) are shown in Fig. 5. This multi-value characteristic can be used to switch motion state of the system. Variation in state parameters (i.e., q_{11} and $\dot{q}_{11}$) enables system to switch from one periodic

Analysis reveals that parameters $\overline{F}_{x_0}$, $\overline{F}_{x_1}$, $\overline{F}_Q$ and $\varepsilon\sigma_2$ all affect periodic motions of the system. Here $\overline{F}_Q$ and $\varepsilon\sigma_2$ are selected as an example to identify the periodic motion of the system with the variation of parameters, namely, subharmonic resonance, principal parametric resonance and coupling resonance. Variation pattern of bifurcation points under different periodic motions is further analyzed. The same rule also applies to influences of $\overline{F}_{x_0}$ and $\overline{F}_{x_1}$ on periodic motions of the system.

In Fig. 6, three bifurcation curves (I, II and III) divide the parametric plane into seven regions. Region A is single-valued, where system has one stable periodic solution while $\overline{F}_Q$ and $\varepsilon\sigma_2$ locate in this region. Regions B, C and D are three-valued, where system has two stable periodic solutions and one unstable periodic solution. Region E and F are five-valued, where system exhibits five periodic solutions (three

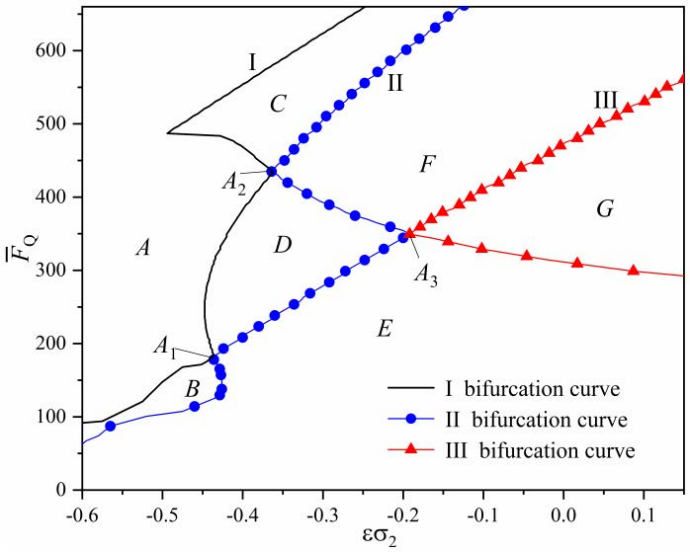

Fig. 6. Bifurcation curves for periodic solutions.

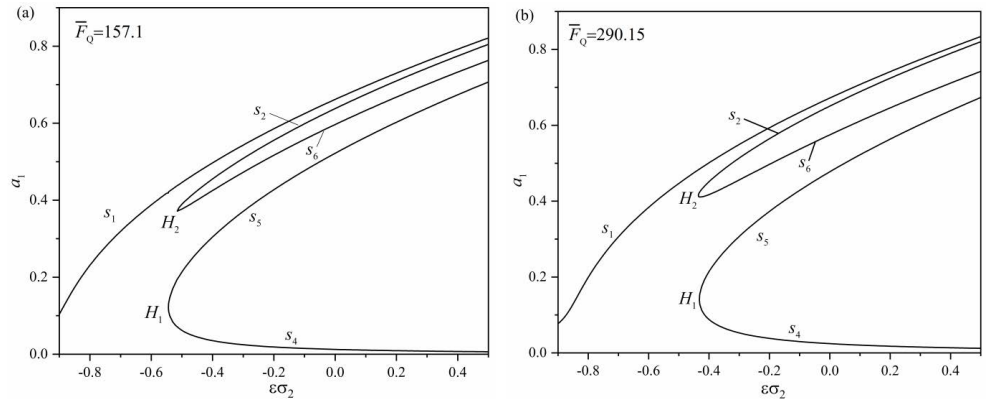

Fig. 7. Amplitude-frequency curves.

stable solutions and two unstable solutions). When $\overline{F}_Q$ and $\varepsilon\sigma_2$ enter into region G, motion of the system becomes most complex while there are four stable periodic solutions and three unstable solutions. Points A_1, A_2 and A_3 are the intersection points of three bifurcation curves. H_1, H_2 and H_3 (Fig. 4) correspond to points on curves I, II and III of Fig. 6, respectively. The detailed analysis of variation trend for these three bifurcation curves (I, II and III) will be presented in subsequent contents.

Changing parameter $\overline{F}_Q$, the amplitude-frequency curves (Fig. 7) are plotted. Observing Fig. 6 and Fig. 7, it is noticed that when the excitation amplitude $\overline{F}_Q$ is relatively small, the subharmonic resonance bifurcation point lies on curve I, the principal parametric resonance bifurcation point lies on curve II and the coupling bifurcation

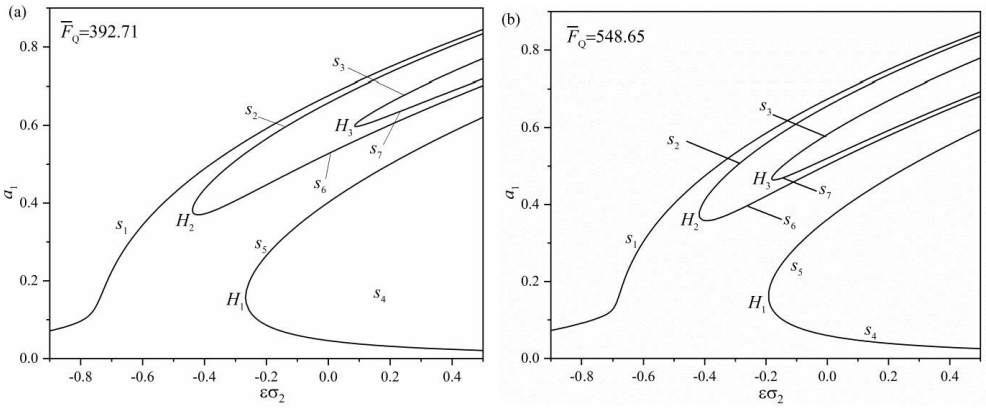

Fig. 8. Amplitude-frequency curves.

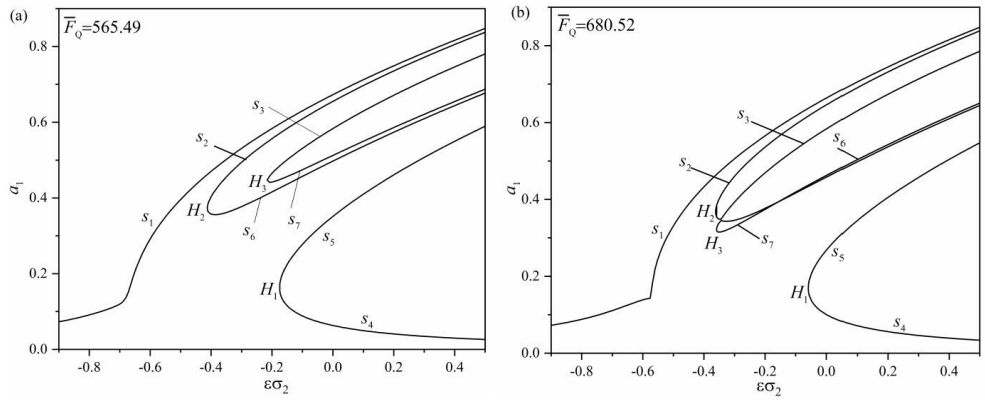

Fig. 9. Amplitude-frequency curves.

point does not appear. As excitation amplitude increases, both point H_1 and point H_2 move to the right, but point H_1 moves faster. When $\overline{F}_Q = 290.15$, the abscissas of point H_1 and point H_2 are the same (Fig. 7b), curves I and II intersect at point A_1 (Fig. 6) where bifurcation occurs to the system, and number of periodic solutions jumps from one to five. As $\overline{F}_Q$ continues to increase, point H_2 locates on curve I and point H_1 locates on curve II, bifurcation point H_3 appears and moves rapidly leftward. When $\overline{F}_Q$ increases to 548.65, the abscissas of point H_1 and H_3 are the same (Fig. 8b), curves II and III intersect at point A_3 (Fig. 6), and number of periodic solutions jumps from three to seven. As $\overline{F}_Q$ continue to increase, point H_1 and point H_2 move rightward, point H_3 overtakes point H_1 and keeps moving leftward. At point A_2 (Fig. 6), the abscissas of point H_2 and point H_3 are the same (Fig. 9b), and curves I and II intersect again. Then with the increase of $\overline{F}_Q$, point H_3 surpasses point H_2 and continues to move to the left. At this moment, point H_3 lies on the curve I, point H_2 is on curve II and point H_1 locates on curve III. Above-mentioned analysis shows that the emergence sequence of subharmonic resonance bifurcation point (point H_1), principal parametric resonance bifurcation point (point H_2) and coupled resonance bifurcation point (point H_3) is closely related to parameters $\overline{F}_Q$ and $\varepsilon\sigma_2$. At some special points (A_1, A_2 and A_3), two kinds of bifurcations occur at the same time, and system displays complicated nonlinear dynamic characteristics.

5 Conclusions

Considering the time-variant tension case, the paper applied analytical and numerical approach to analyze parametric and subharmonic simultaneous resonance of fluid-structure coupling system subjected to follower force, and Lyapunov's stability theory is introduced to determine the stability of periodic solutions of the system.

Through analytical analysis, it is noticed that the influence of excitation amplitude $\overline{F}_Q$ and detuning parameter $\varepsilon\sigma_2$ on the steady-state response of the system is more remarkable, therefore bifurcation curves of periodic solutions on these two parameters are given.

Analysis shows the emergence sequence of three bifurcation points (i.e. principal parametric resonance bifurcation point, subharmonic resonance bifurcation point and coupled resonance bifurcation point) relates closely to $\overline{F}_Q$ and $\varepsilon\sigma_2$, and sometimes two kinds of bifurcations appear at the same time in the system. Adjust of excitation amplitude and detuning parameter enables the system to display different dynamic behaviors, such as subharmonic resonance, principal parametric resonance or simultaneous resonance. This dynamic characteristics make it possible to keep the system in a specific motion state by adjusting the parameters, so to achieve optimization of the system. In the hot-dip galvanizing production line, it is necessary to establish an online control system for the surface quality of steel strips, so to improve the quality of galvanized layer. Results of this paper provide an effective theoretical basis for the online control system.

ACKNOWLEDGMENTS

This work was supported by the National Natural Science Foundation of China (Grant No.11502050 and No.11672072).

REFERENCES

[1] J.A. WICKERT, C.D. MOTE JR. (1990) Classical vibration analysis of axially moving continua. *Journal of Applied Mechanics* **57** 738-744.

[2] W.D. ZHU, B.Z. GUO (1998) Free and forced vibration of an axially moving string with an arbitrary velocity profile. *Journal of Applied Mechanics* **65** 901-907.

[3] G. SUWEKEN, W.T. VAN HORSSEN (2003) On the weakly nonlinear, transversal vibrations of a conveyor belt with a low and time-varying velocity. *Nonlinear Dynamics* **31** 197-223.

[4] J.R. BANERJEE, W.D. GUNAWARDANA (2007) Dynamic stiffness matrix development and free vibration analysis of a moving beam. *Journal of Sound and Vibration* **303** 135-143.

[5] J.L. HUANG, R.K.L. SU, W.H. LI, S.H. CHEN (2011) Stability and bifurcation of an axially moving beam tuned to three-to-one internal resonances. *Journal of Sound and Vibration* **330** 471-485.

[6] H. DING, L.Q. CHEN (2011) Natural frequencies of nonlinear vibration of axially moving beams. *Nonlinear Dynamics* **63** 125-134.

[7] M.H. GHAYESH, M. AMABILI, M.P. PAÏDOUSSIS (2013) Nonlinear dynamics of axially moving plates. *Journal of Sound and Vibration* **332** 391-406.

[8] M.H. GHAYESH, M. AMABILI (2013) Non-linear global dynamics of an axially moving plate. *International Journal of Non-Linear Mechanics* **57** 16-30.

[9] X.Y. MAO, H. DING, L.Q. CHEN (2017) Forced vibration of axially moving beam with internal resonance in the supercritical regime. *International Journal of Mechanical Sciences* **131-132** 81-94.

[10] K. MARYNOWSKI, J. GRABSKI (2013) Dynamic analysis of an axially moving plate subjected to thermal loading. *Mechanics Research Communications* **51** 67-71.

[11] Y.F. ZHOU, Z.M. WANG (2019) Dynamic instability of axially moving viscoelastic plate. *European Journal of Mechanics / A Solids* **73** 1-10.

[12] M. PAKDEMIRLI, H.R. ÖZ (2008) Infinite mode analysis and truncation to resonant modes of axially accelerated beam vibrations. *Journal of Sound and Vibration* **311** 1052-1074.

[13] M.H. GHAYESH (2011) Nonlinear forced dynamics of an axially moving viscoelastic beam with an internal resonance. *International Journal of Mechanical Sciences* **53** 1022-1037.

[14] X.Y. MAO, H. DING, L.Q. CHEN (2019) Internal resonance of a supercritically axially moving beam subjected to the pulsating speed. *Nonlinear Dynamics* **95** 631-651.

[15] Y.Q. TANG, L.Q. CHEN (2012) Primary resonance in forced vibrations of in-plane translating viscoelastic plates with 3:1 internal resonance. *Nonlinear Dynamics* **69** 159-172.

[16] Y.F. ZHOU, Z.M. WANG (2019) Dynamic instability of axially moving viscoelastic plate. *European Journal of Mechanics / A Solids* **73** 1-10.

[17] S.F. LU, N. XUE, W. ZHANG, X.J. SONG, W.S. MA (2021) Dynamic stability of axially moving graphene reinforced laminated composite plate under constant and varied velocities. *Thin-Walled Structures* **167** 1-13.

[18] J.P. SONG, G.L. SHE (2023) Nonlinear resonance of axially moving GPLRMF plates with different boundary conditions. *Structural Engineering and Mechanics* **86** 361-371.

[19] M.H. GHAYESH (2012) Coupled longitudinal–transverse dynamics of an axially accelerating beam. *Journal of Sound and Vibration* **331** 5107-5124.

[20] Y.Q. TANG, D.B. ZHANG, J.M. GUO (2016) Parametric and internal resonance of axially accelerating viscoelastic beams with the recognition of longitudinally varying tensions. *Nonlinear Dynamics* **83** 401-418.

[21] X.Y. MAO, H. DING, L.Q. CHEN (2017) Dynamics of a super-critically axially moving beam with parametric and forced resonance. *Nonlinear Dynamics* **89** 1475-1487.

[22] B. SAHOO, L.N. PANDA, G. POHIT (2015) Two-frequency parametric excitation and internal resonance of a moving viscoelastic beam. *Nonlinear Dynamics* **82** 1721-1742.

[23] B. SAHOO, L.N. PANDA, G. POHIT (2016) Combination, principal parametric and internal resonances of an accelerating beam under two frequency parametric excitation. *International Journal of Non-Linear Mechanics* **78** 35-44.

[24] B. SAHOO (2020) Nonlinear dynamics of a viscoelastic beam traveling with pulsating speed, variable axial tension under two-frequency parametric excitations and internal resonance. *Nonlinear Dynamics* **99** 945-979.

[25] D.B. ZHANG, Y.Q. TANG, H. DING, L.Q. CHEN (2019) Parametric and internal resonance of a transporting plate with a varying tension. *Nonlinear Dynamics* **98** 2491-2508.

[26] Y.D. HU, J.Z. ZHANG (2013) Principal parametric resonance of axially accelerating rectangular thin plate in magnetic field. *Applied Mathematics and Mechanics* **34** 1405-1420.

[27] G. YAO, Z.B. XIE, L.S. ZHU, Y.M. ZHANG (2021) Nonlinear vibrations of an axially moving plate in aero-thermal environment. *Nonlinear Dynamics* **105** 2921-2933.

[28] W. LIN, N. QIAO (2008) Vibration and stability of an axially moving beam immersed in fluid. *International Journal of Solids and Structures* **45** 1445-1457.

[29] Y. HAO, H.L. DAI, Q. NI, K. ZHOU, L. WANG (2020) Dynamics and stability analysis of an axially moving beam in axial flow. *Journal Mechanics of Materials and Structures* **15** 37-60.

[30] Y.Q. WANG, H. WU, F.L. YANG, Q. WANG (2021) An efficient method for vibration and stability analysis of rectangular plates axially moving in fluid. *Applied Mathematics and Mechanics* **42** 291-308.

[31] X.X. GUO, Z.M. WANG, Y. WANG (2011) Dynamic stability of thermoelastic coupling moving plate subjected to follower force. *Applied Acoustics* **72** 100-107.

[32] Y. WANG, T. JING, J.M. WU, M. XIE (2015) Stability of axially moving piezolaminated viscoelastic plate subjected to follower force. *Advances in Materials Science and Engineering* **2015** Article ID 758472, 12 pages.

[33] J. LI, X.H. GUO, J. LUO, H.Y. LI, ET AL. (2013) Analytical study on inherent properties of a unidirectional vibrating steel strip partially immersed in fluid. *Shock and Vibration* **20** 793-807.

[34] H.Y. LI, J. LI, Y.J. LIU (2015) Internal resonance of an axially moving unidirectional plate partially immersed in fluid under foundation displacement excitation. *Journal of Sound and Vibration* **358** 124-141.

[35] H.Y. LI, T.Y. LANG, Y.J. LIU, J. LI (2019) Nonlinear vibrations and stability of an axially moving plate immersed in fluid. *Acta Mechanica Solida Sinica* **32** 737-753.

[36] M. AMABILI (2008) "Nonlinear Vibrations and Stability of Shells and Plates". Cambridge University Press, New York.

[37] Y.Q. WANG, X.B. HUANG, J. LI (2016) Hydroelastic dynamic analysis of axially moving plates in continuous hot-dip galvanizing process. *International Journal of Mechanical Sciences* **110** 201-216.

[38] A.H. NAYFEH (1981) "Introduction to Perturbation Techniques". John Wiley and Sons, New York.

[39] A. ABE, Y. KOBAYASHI, G. YAMADA (1998) Analysis of subharmonic resonance of moderately thick antisymmetric angle-ply laminated plates by using method of multiple scales. *Journal of Sound and Vibration* **217** 467-484.

[40] M.R. PERMOON, H. HADDADPOUR, M. JAVADI (2018) Nonlinear vibration of fractional viscoelastic plate: Primary, subharmonic, and superharmonic response. *International Journal of Non-Linear Mechanics* **99** 154-164.